35th Annual International Conference of the IEEE EMBS
Osaka, Japan, 3 - 7 July, 2013

Extraction of Intended Palpation Times from Facial EMGs in a Mouse Model of Active Sensing

Joseph B. Schroeder* and Jason T. Ritt*

*Department of Biomedical Engineering
Boston University, Boston, Massachusetts 02215
jbs7@bu.edu, jritt@bu.edu

Abstract— **The rodent whisker system is a common model for somatosensory neuroscience and sensorimotor integration. In support of ongoing efforts to assess neural stimulation approaches for future sensory prostheses, in which we deliver optogenetic stimulation to the somatosensory cortex of behaving mice, we must coordinate feedback in real time with active sensing whisker motions. Here we describe methods for extracting the times of whisker palpations from bilateral bipolar facial electromyograms (EMG). In particular, we show onset times extracted offline from EMG envelopes lead whisker motion onsets extracted from high speed video (HSV) by ≈ 16 ms. While HSV provides ground truth for sensing motions, it is not a feasible source of real time information suitable for neurofeedback experiments. As an alternative, we find the temporal derivative of the EMG envelope reliably predicts whisker motion onsets with short latency. Thus EMG, although providing noisy and partial information, can serve well as an input to control algorithms for testing neural processing of active sensing information, and providing stimulation for artificial touch experiments.**

I. INTRODUCTION

The rodent whisker system is a highly studied and well established model for sensorimotor neuroscience [1], [2] with relevance to brain machine interfaces (BMI) and sensory neuroprosthetics [3]–[5]. Rats and mice rapidly palpate objects with their whiskers using specialized musculature in their face [6], [7], in a ≈10 Hz oscillatory motion known as whisking [7], and this robust active sensing behavior is increasingly studied as an analog to active touch in humans [8], [9]. While high speed videography is the gold standard method for recording whisker motions [7], [10]–[16], current automated tracking methods are computationally intensive, lack robustness across viewing conditions, and may be difficult to apply in real time settings such as those required in BMI experiments. A more immediately available signal comes from facial electromyography (EMG), which has been used in rats to track the timing of whisks [17]–[20]. Methodology for mice has lagged that for rats, in part because of the difficulty of making devices small and light enough for animals an order of magnitude smaller [21], [22]. Here we describe adaptation of EMG recording and signal processing methods to mice, and demonstrate the effectiveness of our approach to extracting times of whisks in a way readily applicable to implementation in real time feedback systems for sensory neuroprosthetic and neurostimulation research.

II. METHODS

A. Electrode Construction and Implantation

We developed bipolar electrodes, implant techniques, and signal processing for facial electromyography (EMG) in behaving mice, adapting methods previously reported for rats [17]–[19]. Each EMG electrode consists of a bipolar, twisted pair electrode constructed using insulated 50 μm stainless steel wire (A-M System, part #790500). The lower stiffness of stainless steel, compared to tungsten used in the above rat studies, placed less mechanical strain on the smaller mouse mystacial pad. We heat fused a twisted pair of wires, whose contacts were spaced approximately 1 mm to try to match an effective dipole of the aggregate muscle activity across the pad. EMG electrodes were implanted in the same surgical procedure as previously described hyperdrives for cortical recording and optical stimulation [21]. The electrodes were placed inside a needle (23ga), subdermal from the anterior edge of the scalp incision and through the facial pad. The needle was removed and the electrodes retracted until the distal tips were just under the pad. Electrode placement targeted the larger posterior whiskers, and was confirmed by eliciting small whisker motions under current stimulation (10 Hz, biphasic, 50% duty cycle, ≈ 100 μA). The electrodes were secured to the skull with dental acrylic. A posterior skull screw provided electrical ground. All procedures were approved by Boston University IACUC.

B. Behavioral arena

Prior to implant, water restricted animals were trained to traverse a 31 cm by 9 cm polycarbonate track in alternating directions to receive water reward. Post-implant sessions were conducted in a sound and light isolated cabinet under IR illumination to minimize external sensory cues. Once trained, mice consistently completed > 100 trials in a 45 minute session. Trials lasted approximately 2 seconds and contained 30-40 whisks.

C. High speed videography

A subset of trials were recorded at 500 frames per second by high speed video (HSV; pco.1200hs camera, Cooke Corporation), through a mirror underneath the transparent track. Five to ten clips per session could be saved to disk due to data rate limitations; in order to avoid selection bias, clips were saved as soon as the previous save completed. For

978-1-4577-0216-7/13/$26.00 ©2013 IEEE

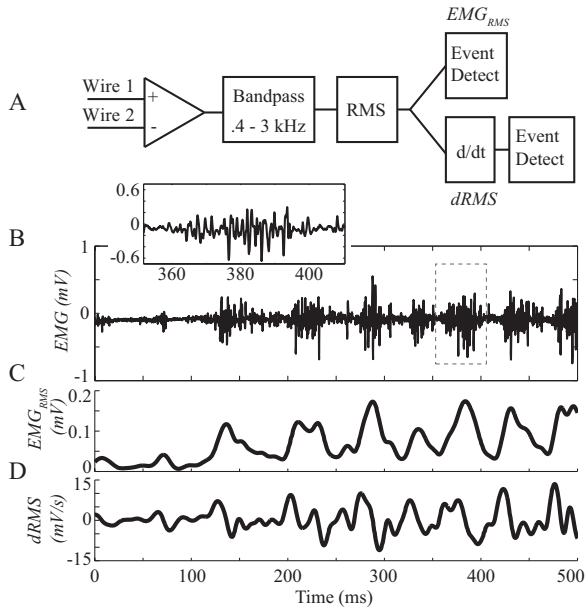

Fig. 1. The signal processing chain for facial EMG. A: Block diagram. The differential recording is bandpassed, and the envelope found as the RMS using a 10 ms Gaussian. The derivative of the RMS is also formed. B: Example of raw EMG signal. Inset shows a zoom of the signal within the dashed box. C: Example of EMG_{RMS} used for offline event detection. D: Example of *dRMS* signal used for real time event detection.

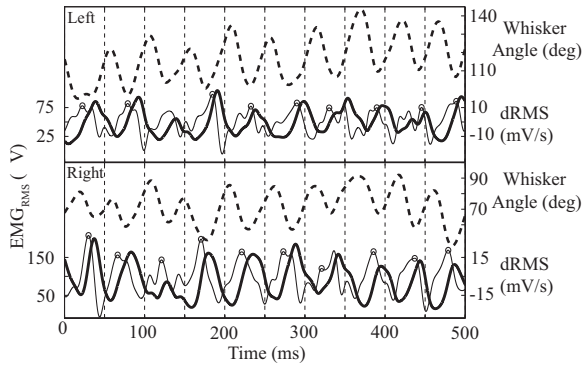

Fig. 2. Example comparison of left and right EMG_{RMS} (thick line) and *dRMS* (thin line) to HSV whisker angles (dashed line). *dRMS* peaks (open circles) tend to occur near the onset of whisker angle increase (protractions).

comparison to EMG, whisker position was manually scored from the HSV using a custom Matlab GUI. For preliminary studies, a single user tracked the position of a single large, posterior whisker on each side of the face (typically C2), and the position of the tips of the nose and mouth. The angle of each whisker was determined relative to the snout, with 180 degrees indicating full protraction and 0 degrees indicating full retraction. Whisker angles were smoothed with a Gaussian kernel (10 ms width) before further analysis.

D. Signal Acquisition

A digital signal processor based acquisition system (RZ2, Tucker David Technologies) collected all signals at 24.4 kHz sampling rate. The tether from a 32 channel headstage at the implant ran through an overhead motorized commutator, to facilitate animal movement, before connecting to a preamp and AD converter (PZ2, TDT). Recorded signals consisted of 4 EMG contacts (bilateral bipolar electrodes) and 24 cortical electrodes. The system also collected timing of camera synchronization and IR beambreak signals (used to track mouse position), and drove reward delivery.

III. RESULTS

A primary motivation to validate EMG as a measure of whisker motion is to enable the use of EMG for real time feedback and neurostimulation applications [23], in place of more demanding whisker tracking derived from HSV. In general EMG does not report the true angle of the whisker to the face [18], but in some neurostimulation contexts, finding the onset times of whisks may be adequate. We therefore focused on signal processing conducive to detection of whisk onsets (block diagram in Fig. 1A). We estimated the envelope of EMG activity, EMG_{RMS} , as the root-mean-square (RMS, computed with a 10 ms width Gaussian kernel) of the bandpassed differential of the bipolar electrode (all steps computed digitally). Fig. 1B shows an example half second segment of the differential signal, during a transition from quiescence to whisking, with EMG_{RMS} shown below (Fig. 1C). EMG_{RMS} was used for offline (non-causal) comparison of EMG to HSV whisker motion estimates. However, to predict individual whisk onsets, we found it useful to take the derivative of the RMS signal (*dRMS* ; Fig. 1D), which eliminated low frequency plateaus that develop over bouts of whisks and disrupt threshold detection. *dRMS* is simple to calculate and robust, and may be more useful for real time processing than the RMS itself.

Comparison of EMG_{RMS} to the videographically reconstructed angle shows the typical relationship between the two measures of whisker motion (Fig. 2). Peaks in EMG_{RMS} occur near valleys in the angle (maximal retractions), indicating that EMG_{RMS} generally rises prior to each whisk, consistent with the expectation that facial EMG arises primarily from "extrinsic" muscles responsible for (forward moving) whisker protractions [18], [19] To quantify the latency from EMG_{RMS} to whisker motion, we identified local extrema in both timeseries offline (using zero-phase non-causal filters). We then computed the amplitude from each minimum to its adjacent local maximum, and eliminated small events for noise rejection (inclusion criteria computed separately: angular displacement $\geq 7^o$, EMG_{RMS} displacement $\geq 50\%$ above the median event computed over all recorded events). Fig. 3A demonstrates this peak and valley identification, with open and closed circles respectively. Visual inspection confirms that the majority of EMG peaks and angle deflections in this session were identified correctly. We calculated the EMG-angle latency as the time from the EMG_{RMS} valley preceding each angular valley. The latency distributions for both sides of the face are presented in Fig. 3B. The median delay values were 16.5 ms (left) and 16.0 ms (right).

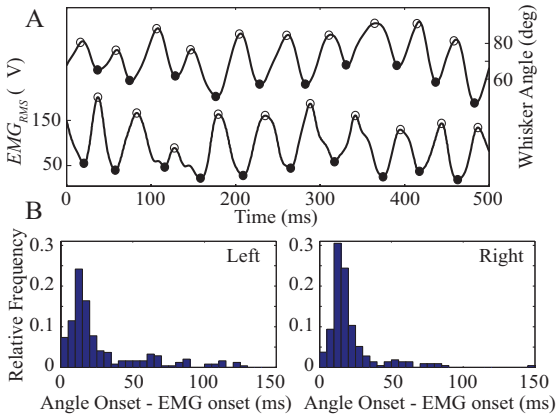

Fig. 3. Offline analysis of EMG timing. A: Example of 0.5 sec of EMG_{RMS} and whisker angle with onsets (valleys) identified by filled circles, and peaks by open circles. B: This peak/valley identification was used to quantify EMG timing (1 mouse, 6 HSV trials). Histograms show the latency from EMG_{RMS} onset to whisk onset for left (n=244 events) and right (n=213 events) whiskers respectively. Median latencies for left and right are 16.5 ms and 16.0 ms.

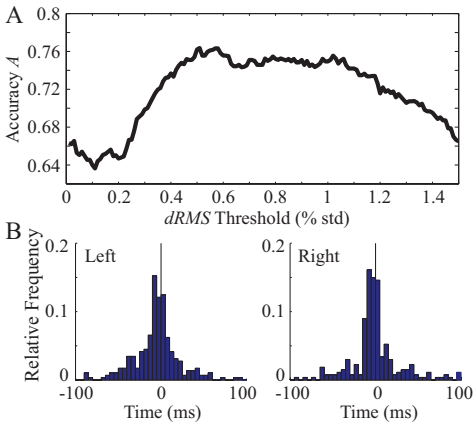

Fig. 4. *dRMS* peaks predict whisk onsets. A: The prediction accuracy from 1 for a range of *dRMS* threshold values, normalized to *dRMS* standard deviations above the mean (over all trials). Comparable results are obtained over a wide range of threshold values between 0.5 and 1.0. B: Histograms show the time from each *dRMS* event to the nearest angle onset for left (n=289) and right (n=269) whiskers. Given that a *dRMS* event occurred, the probability of an angular onset within ± 25 ms was 71.3% and 70.0% for the two sides. (1 mouse, 6 HSV trials).

The preceding analysis shows the behavioral relevance of the EMG signals, and quantifies the latency from electrical events to muscle contraction inherent in the physiology of muscle activation. However, we desire a method that will enable real time predictions of angular onsets given the EMG. Since whisker palpations begin with fast forward acceleration, and our recordings are preferentially sensitive to muscles driving this motion, we observed that high narrow peaks in *dRMS* appeared temporally close to whisk onsets as determined from HSV. Peaks in the *dRMS* signal were identified as local maxima between successive upward and downward crossings of *dRMS* through a positive threshold. Additionally, we imposed a refractory period of 25 ms to suppress high frequency noise contamination in the threshold crossings. In order to evaluate the effectiveness of this method at predicting angular motion onsets given *dRMS* information, we define a measure, A, of prediction accuracy as:

$$A = \frac{\#\text{ detected angle onsets}}{1/2[(\#\text{ total angle onsets}) + (\#dRMS\text{ peaks})]} \quad (1)$$

The numerator is the total number of HSV-determined whisk onsets that fell within ± 25 ms of a *dRMS* peak. The denominator normalizes these correct detections by the total number of whisk onsets and the total number of *dRMS* peaks. Perfect detection of whisk onsets without any superfluous *dRMS* peaks would produce $A = 1$. Whisk onsets that are missed, have multiple *dRMS* peaks associated with them, or *dRMS* peaks in the absence of whisking would all reduce A. A central question in detection of whisks by *dRMS* peaks is choice of threshold. We determined the selection of threshold for *dRMS* peak identification by evaluating Eqn. (1) over a range of thresholds (mean(*dRMS*) + X * std(*dRMS*), where X ranged from 0 to 1.5). As shown in Fig. 4A, the predictive accuracy is largely flat for thresholds between 0.5 and 1.0. Accuracy diminished outside this range. Lower thresholds introduced too many spurious *dRMS* peaks, while larger thresholds missed peaks corresponding to true whisk onsets. Based on the curve in Fig. 4A, a threshold of 0.75 STDs above the mean was selected. Using this threshold, the probability of having a whisk onset within ± 25 ms of a detected *dRMS* peak was 71.3% (left) and 70.0% (right). The time between each identified *dRMS* peak and the nearest whisk onset, which also measured predictive accuracy, is shown in Fig. 4B. The median time from *dRMS* peak to the nearest whisk onset was 10.8 ms (left) and 10.6 ms (right).

IV. CONCLUSIONS

We have demonstrated a reliable detector of whisker motion onsets in mice using facial EMG. Peaks in EMG_{RMS} predict an onset of angular motion approximately 16 ms later, a latency from the first detectable electrical signal to the first observable motion well within the computational speed available to real time feedback systems for experiments in sensory prosthetics under active sensing ($\approx$ 1 ms) [3]. The ability to use facial EMGs as a surrogate for whisker motions is significant because it reduces the emphasis that must be placed on manual whisker tracking in HSV. This enables real time access to information on motion onsets and allows for analysis of all trials rather than the subset captured by HSV. We further demonstrated that the temporal derivative *dRMS* of EMG_{RMS} provides a reliable indicator of an impending whisk onset. Since the derivative is just a scaled version of the two-sample difference, this method can be used in real time, and is subject only to user-configurable latencies needed to define local maxima. With causal filters, there will be an additional small ($\approx$ 5 ms) latency due to the high pass filter placed before the rectifier. Since EMG activation precedes angular motion onset, this method enables control strategies that involve providing

neural stimulation before whisking motion occurs. Future experiments will seek to leverage this capability to deliver cell type specific optogenetic stimulation [24] that is precisely timed relative to whisker motions. For example, to activate inhibitory networks in primary somatosensory cortex prior to and continuing through whisker motion onset could clarify the strength, cellular origin and timing of thalamocortical "windows of opportunity" for integrating sensory inputs in the cortex [25].

The most significant limitation of this method is that limited information is available about absolute whisker angle. In some cases, we observed a slight positive correlation between the smoothed magnitude of *dRMS* (100 ms wide Gaussian kernel) and the magnitude of angular deflection occurring in the 25 ms following peaks detected in the original *dRMS* signal (data not shown). This correlation was not sufficiently robust to predict angular information from *dRMS* signals. Although the relationship between EMG amplitudes and angle deflections remains an important direction for future work, we concentrated on determining activation times and the relative timing of EMG and whisker motion, which are robust and may be adequate in many settings. Additionally, EMG recordings can be corrupted by artifacts from motion, sniffing, or other non-whisker muscle activation. It is important to note that no subselection has been done in this study for periods in which the mouse was actively whisking. In other words, our estimates of prediction accuracy reflect a reasonable summary of how the method would perform over a range of animal behaviors not known in advance. Examining only periods of large amplitude whisking would significantly increase the performance of our prediction method. A key strength of the current method is that it is relatively insensitive to the choice of *dRMS* threshold. While thresholds may be set daily in a short calibration epoch if required, we observed EMG amplitudes to be highly consistent from day to day and found small errors in threshold selection to have a minor impact.

We have demonstrated that electromyographic recording techniques can be successfully adapted for use in the much smaller facial pads of mice, and that EMG provides a robust indication of palpation onsets. This technique provides an important tool to facilitate experiments in actively behaving mice to develop feedback interfaces for sensory prosthetics.

V. ACKNOWLEDGMENTS

J. T. R. holds a Career Awards at the Scientific Interface from the Burroughs Wellcome Fund.

REFERENCES

[1] C. C. H. Petersen, "The Functional Organization of the Barrel Cortex," *Neuron*, vol. 56, no. 2, pp. 339–355, 2007.

[2] D. Feldmeyer, M. Brecht, F. Helmchen, C. C. H. Petersen, J. F. A. Poulet, J. F. Staiger, H. J. Luhmann, and C. Schwarz, "Barrel cortex function." *Progress in Neurobiology*, 2012.

[3] S. Venkatraman and J. M. Carmena, "Active sensing of target location encoded by cortical microstimulation." *IEEE Trans. Neural Sys. Rehab. Eng.*, vol. 19, no. 3, pp. 317–324, 2011.

[4] S. K. Talwar, S. Xu, E. S. Hawley, S. A. Weiss, K. A. Moxon, and J. K. Chapin, "Rat navigation guided by remote control." *Nature*, vol. 417, no. 6884, pp. 37–38, 2002.

[5] S. Butovas, S. G. Hormuzdi, H. Monyer, and C. Schwarz, "Effects of electrically coupled inhibitory networks on local neuronal responses to intracortical microstimulation." *Journal of Neurophysiology*, vol. 96, no. 3, pp. 1227–1236, 2006.

[6] J. Dörfl, "The musculature of the mystacial vibrissae of the white mouse." *J. Anatomy*, vol. 135, no. 1, pp. 147–154, 1982.

[7] B. Mitchinson, R. A. Grant, K. Arkley, V. Rankov, I. Perkon, and T. J. Prescott, "Active vibrissal sensing in rodents and marsupials." *Phil. Trans. Roy. Soc. B: Biol. Sci.*, vol. 366, no. 1581, pp. 3037–3048, 2011.

[8] G. Horev, A. Saig, P. M. Knutsen, M. Pietr, C. Yu, and E. Ahissar, "Motor-sensory convergence in object localization: a comparative study in rats and humans," *Phil. Trans. Roy. Soc. B: Biol. Sci.*, vol. 366, no. 1581, pp. 3070–3076, 2011.

[9] M. E. Diamond, "Texture sensation through the fingertips and the whiskers," *Curr. Opin. Neurobiol.*, vol. 20, no. 3, pp. 319–327, 2010.

[10] J. T. Ritt, M. L. Andermann, and C. I. Moore, "Embodied information processing: vibrissa mechanics and texture features shape micromotions in actively sensing rats." *Neuron*, vol. 57, no. 4, pp. 599–613, 2008.

[11] J. Ritt, "High speed videography of embodied active sensing in the rodent whisker system," *Springer Methods: Neuronal Network Analysis*, 2011.

[12] J. Voigts, B. Sakmann, and T. Celikel, "Unsupervised whisker tracking in unrestrained behaving animals." *Journal of Neurophysiology*, vol. 100, no. 1, pp. 504–515, 2008.

[13] P. M. Knutsen, D. Derdikman, and E. Ahissar, "Tracking whisker and head movements in unrestrained behaving rodents." *Journal of Neurophysiology*, vol. 93, no. 4, pp. 2294–2301, 2005.

[14] N. G. Clack, D. H. O'Connor, D. Huber, L. Petreanu, A. Hires, S. Peron, K. Svoboda, and E. W. Myers, "Automated tracking of whiskers in videos of head fixed rodents." *PLoS Computational Biology*, vol. 8, no. 7, p. e1002591, 2012.

[15] I. Perkon, A. Kosir, P. M. Itskov, J. Tasic, and M. E. Diamond, "Unsupervised quantification of whisking and head movement in freely moving rodents." *Journal of Neurophysiology*, vol. 105, no. 4, pp. 1950–1962, 2011.

[16] R. B. Towal and M. J. Hartmann, "Right-left asymmetries in the whisking behavior of rats anticipate head movements." *Journal of Neuroscience*, vol. 26, no. 34, pp. 8838–8846, 2006.

[17] G. E. Carvell, D. J. Simons, S. H. Lichtenstein, and P. Bryant, "Electromyographic activity of mystacial pad musculature during whisking behavior in the rat." *Somatosensory & Motor Research*, vol. 8, no. 2, pp. 159–164, 1991.

[18] R. W. Berg and D. Kleinfeld, "Rhythmic whisking by rat: retraction as well as protraction of the vibrissae is under active muscular control," *Journal of Neurophysiology*, vol. 89, no. 1, pp. 104–117, 2003.

[19] D. N. Hill, R. Bermejo, H. P. Zeigler, and D. Kleinfeld, "Biomechanics of the vibrissa motor plant in rat: rhythmic whisking consists of triphasic neuromuscular activity." *Journal of Neuroscience*, vol. 28, no. 13, pp. 3438–3455, 2008.

[20] B. Mitchinson, C. J. Martin, R. A. Grant, and T. J. Prescott, "Feedback control in active sensing: rat exploratory whisking is modulated by environmental contact," *Proceedings of the Royal Society B: Biological Sciences*, vol. 274, no. 1613, pp. 1035–1041, 2007.

[21] J. H. Siegle, M. Carlen, K. Meletis, L.-H. Tsai, C. I. Moore, and J. Ritt, "Chronically implanted hyperdrive for cortical recording and optogenetic control in behaving mice." *Conference proceedings of the IEEE Engineering in Medicine and Biology Society.*, vol. 2011, pp. 7529–7532, 2011.

[22] M. M. Halassa, J. H. Siegle, J. T. Ritt, J. T. Ting, G. Feng, and C. I. Moore, "Selective optical drive of thalamic reticular nucleus generates thalamic bursts and cortical spindles," *Nat. Neurosci.*, vol. 14, no. 9, pp. 1118–1120, 2011.

[23] Y. Ahmadian, A. M. Packer, R. Yuste, and L. Paninski, "Designing optimal stimuli to control neuronal spike timing," *Journal of Neurophysiology*, vol. 106, no. 2, pp. 1038–1053, 2011.

[24] L. Fenno, O. Yizhar, and K. Deisseroth, "The Development and Application of Optogenetics," *Annual Review of Neuroscience*, vol. 34, no. 1, pp. 389–412, 2011.

[25] D. J. Pinto, J. C. Brumberg, and D. J. Simons, "Circuit dynamics and coding strategies in rodent somatosensory cortex." *Journal of Neurophysiology*, vol. 83, no. 3, pp. 1158–1166, 2000.